AMERICAN SOCIETY FOR MICROBIOLOGY | Molecular and Cellular Biology

A MARCH6 and IDOL E3 Ubiquitin Ligase Circuit Uncouples Cholesterol Synthesis from Lipoprotein Uptake in Hepatocytes

Anke Loregger,[a] Emma Claire Laura Cook,[a] Jessica Kristin Nelson,[a] Martina Moeton,[a] Laura Jane Sharpe,[c] Susanna Engberg,[d] Madina Karimova,[d] Gilles Lambert,[b] Andrew John Brown,[c] Noam Zelcer[a]

Department of Medical Biochemistry, Academic Medical Center, University of Amsterdam, Amsterdam, The Netherlands[a]; Laboratoire Inserm UMR 1188, Université de la Réunion, Sainte-Clothilde, France[b]; School of Biotechnology and Biomolecular Sciences, The University of New South Wales, Sydney, NSW, Australia[c]; AstraZeneca R&D, Gothenburg, Sweden[d]

Cholesterol synthesis and lipoprotein uptake are tightly coordinated to ensure that the cellular level of cholesterol is adequately maintained. Hepatic dysregulation of these processes is associated with pathological conditions, most notably cardiovascular disease. Using a genetic approach, we have recently identified the E3 ubiquitin ligase MARCH6 as a regulator of cholesterol biosynthesis, owing to its ability to promote degradation of the rate-limiting enzymes 3-hydroxy-3-methyl-glutaryl coenzyme A reductase (HMGCR) and squalene epoxidase (SQLE). Here, we present evidence for MARCH6 playing a multifaceted role in the control of cholesterol homeostasis in hepatocytes. We identify MARCH6 as an endogenous inhibitor of the sterol regulatory element binding protein (SREBP) transcriptional program. Accordingly, loss of *MARCH6* increases expression of SREBP-regulated genes involved in cholesterol biosynthesis and lipoprotein uptake. Unexpectedly, this is associated with a decrease in cellular lipoprotein uptake, induced by enhanced lysosomal degradation of the low-density lipoprotein receptor (LDLR). Finally, we provide evidence that induction of the E3 ubiquitin ligase IDOL represents the molecular mechanism underlying this MARCH6-induced phenotype. Our study thus highlights a MARCH6-dependent mechanism to direct cellular cholesterol accretion that relies on uncoupling of cholesterol synthesis from lipoprotein uptake.

Cholesterol is an essential constituent of cellular membranes and signaling pathways and is a precursor of sterol-derived molecules (1). Yet elevated levels of cholesterol are toxic to cells, and dysregulated cholesterol metabolism is associated, most evidently, with development of cardiovascular disease. As such, multiple transcriptional networks and posttranscriptional processes regulate the synthesis, uptake, and efflux of cholesterol. Transcriptionally, these processes are largely governed by the opposing actions of the transcription factors sterol regulatory element binding proteins (SREBPs) and the liver X receptors (LXRs) (2–6). Upon sensing low cholesterol levels in the endoplasmic reticulum (ER), SREBPs are processed into their mature, transcriptionally active form. This results in induction of the full set of genes required for *de novo* biosynthesis of cholesterol via the mevalonate pathway and of the low-density lipoprotein receptor (LDLR) that is required for uptake of LDL-derived cholesterol (7, 8). In contrast, LXRs, members of the nuclear receptor family, are activated when cellular cholesterol levels are elevated. Once activated by their cognate oxysterol ligands, LXRs induce cholesterol efflux pathways (e.g., via the transporters ABCA1 and ABCG1) and limit LDL uptake by inducing expression of the E3 ubiquitin ligase (E3)-inducible degrader of the LDLR (IDOL) (6, 9, 10). The coordinated action of these two transcription factor families ensures that cellular cholesterol is adequately maintained at an appropriate level.

Next to transcriptional regulation, posttranscriptional mechanisms are emerging as a potent method to regulate cholesterol metabolism. Here, ubiquitylation-stimulated degradation of key nodes of cellular cholesterol metabolism is often used (11). Two notable examples are the sterol-dependent ubiquitylation of the LDLR by IDOL and of the rate-limiting enzyme in the mevalonate pathway, 3-hydroxy-3-methyl-glutaryl coenzyme A reductase (HMGCR), by two ER-resident E3s, GP78 and TRC8 (12–14). Following their ubiquitylation, the LDLR and HMGCR are subjected to degradation in the lysosome and to ER-associated degradation (ERAD) in the proteasome, respectively. We along with others have recently identified the ER-resident E3 membrane-associated RING Finger 6, MARCH6 (also known as TEB4), as an E3 that controls the basal and cholesterol-stimulated degradation of squalene epoxidase (SQLE; also known as squalene monooxygenase) (15–17). Acting downstream of HMGCR, SQLE is a second, less appreciated, rate-limiting step in the mevalonate pathway and, in fact, the enzyme committing the pathway to producing cholesterol rather than isoprenoids (15). In response to elevated cholesterol levels, MARCH6, acting as an ERAD-associated E3, promotes the ubiquitylation and proteasomal degradation of SQLE. This in turn attenuates production of cholesterol through the mevalonate pathway, while sparing isoprenoid synthesis (16, 18).

While MARCH6 controls SQLE abundance, we also found that the silencing of *MARCH6* regulates the basal levels of HMGCR, comparable to what was shown for the E3 HRD1 (16, 19). The ability of MARCH6 to govern the levels of these two important rate-limiting enzymes in cholesterol biosynthesis positions it as a

Received 22 September 2015 **Returned for modification** 20 October 2015
Accepted 27 October 2015

Accepted manuscript posted online 2 November 2015

Citation Loregger A, Cook ECL, Nelson JK, Moeton M, Sharpe LJ, Engberg S, Karimova M, Lambert G, Brown AJ, Zelcer N. 2016. A MARCH6 and IDOL E3 ubiquitin ligase circuit uncouples cholesterol synthesis from lipoprotein uptake in hepatocytes. Mol Cell Biol 36:285–294. doi:10.1128/MCB.00890-15.

Address correspondence to Noam Zelcer, n.zelcer@amc.uva.nl.

Supplemental material for this article may be found at http://dx.doi.org/10.1128/MCB.00890-15.

regulator of metabolic flux through the mevalonate pathway. For SQLE this involves direct ubiquitylation by MARCH6, but the mechanism behind control of HMGCR abundance by MARCH6 is unclear. In the current study, we reveal a multifaceted role for MARCH6 in controlling cholesterol metabolism in hepatocytes. We identify MARCH6 as a negative regulator of SREBP2-mediated transcription and describe an unexpected E3 circuit functionally linking MARCH6 and IDOL to limit uptake of LDL via the LDLR pathway.

MATERIALS AND METHODS

Reagents. Bafilomycin A1 and MG132 were purchased from Calbiochem. Recombinant human proprotein convertase subtilisin/kexin 9 (hPCSK9) was from Invitrogen. Alirocumab, a humanized PCSK9-blocking antibody, was a kind gift from Sanogi-Regeneron. All other reagents were purchased from Sigma.

Cell culture. HEK293T, HepG2, Huh7, and SNB19 cells were obtained from ATCC. HepG2 cells stably expressing LDLR-green fluorescent protein (GFP) were previously described (10). An IDOL HepG2 knockout (KO) cell line was generated by deleting 41 bp in exon 4 using CRISPR/Cas9 technology, and single clones were ultimately analyzed using next-generation sequencing. Cells were cultured at 37°C and 5% CO_2 in Dulbecco's modified eagle's medium (DMEM) supplemented with 10% fetal bovine serum (FBS). IHH cells were a kind gift from Geesje Dallinga-Thie (Amsterdam, The Netherlands) and cultured in William's E medium supplemented with 2 mM glutamine, 10% FBS, 20 mU/ml bovine insulin, and 50 nM dexamethasone, as previously reported (20). Where indicated in the figures and figure legends, cells were sterol depleted by culture in sterol depletion medium (DMEM supplemented with 10% lipoprotein-deficient serum [LPDS], 2.5 μg/ml simvastatin, and 100 μM mevalonate) for 24 h. For detection of PCSK9 in culture medium, cells were washed with phosphate-buffered saline (PBS) and cultured in Opti-MEM (Invitrogen) for 24 h prior to cell lysis. The culture medium was collected, and cell debris was removed by centrifugation.

siRNA interference experiments. To silence specific genes, HEK293T cells were transfected with 30 nM small interfering RNA (siRNA) using JetPrime (Polyplus). HepG2 and Huh7 cells were reverse transfected with 30 nM siRNA using Lipofectamine RNAiMAX (Invitrogen). For cotransfections with plasmids, cells were transfected using JetPrime (Polyplus). To silence two genes (double knockdowns), a 30 nM concentration of each of two siRNAs was used. The total amount of siRNA transfected into cells was kept constant within an experiment. Unless otherwise stated, ON-TARGETplus SMART pool control (D-001810-10), MARCH6 (L-006925-00), and IDOL (L-006976-00) siRNAs from Dharmacon were used. Ambion Silencer Select single MARCH6 siRNAs (catalog numbers S20137, S20138, and S20139) and controls (AM4611) were purchased from Invitrogen and used as indicated in the figures and figure legends.

RNA isolation and qPCR. Total RNA was isolated from cells using a Direct-zol RNA MiniPrep kit (Zymo Research). One microgram of total RNA was reverse transcribed using an iScript cDNA synthesis kit (Bio-Rad). FastStart Sybr green Master (Roche) or SensiFAST SYBR (Bioline) was used for real-time quantitative PCR (qPCR) assays performed on a LightCycler 480 II system (Roche). Gene expression levels were determined and normalized to the expression level of 36B4. Sequences for qPCR primers are available upon request.

Antibodies, immunoblot analysis, and immunoprecipitation. Total cell lysates were prepared in radioimmunoprecipitation assay (RIPA) buffer (150 mM NaCl, 1% NP-40, 0.1% sodium deoxycholate, 0.1% SDS, 100 mM Tris-HCl, pH 7.4) supplemented with protease inhibitors (Roche). Lysates were cleared by centrifugation at 4°C for 10 min at 10,000 × *g*. Samples were separated on NuPAGE Novex 4 to 12% Bis-Tris gels (Invitrogen) and transferred to nitrocellulose membranes. Membranes were probed with antibodies for following: LDLR (EP1553Y, 1:1,000; Abcam), tubulin (clone DM1A, ascitic fluid, 1:5,000; Sigma,), β-actin (1:10,000; Millipore,) very-low-density lipoprotein receptor (VLDLR) (6A6, 1:1,000; Santa Cruz Biotechnology), His (H8, 1:1000; Abcam), squalene monooxygenase (1:500; Proteintech), FLAG (M2, 1:1,000; Sigma), V5 (1:1,000; Invitrogen), and PCSK9 (10240, 1:1,000; Cayman Chemical). Secondary horseradish peroxidase-conjugated antibodies (Invitrogen) were used and visualized with chemiluminescence on a Fuji LAS 4000 system (GE Healthcare). All immunoblots shown are representative of at least three independent experiments with similar results.

Plasmids and expression constructs. The $LDLR_{4000}$-Luc (where Luc is luciferase) and LDLR-Sm-Luc (proximal LDLR promoter in which the SRE is mutated) reporters were a kind gift from Hiroyoshi Ariga (Hokkaido University, Japan) (21). The SRE-Luc and 3-hydroxy-3-methylglutaryl coenzyme A synthase (HMGCS)-Luc reporters were a gift from Joseph Roitelman (Tel Aviv University, Israel). Luciferase reporter assays were performed using a Dual-luciferase reporter assay kit (Promega) according to the manufacturer's instructions. The expression plasmid encoding a C-terminally tagged V5 PCSK9 was constructed by amplification of human PCSK9 cDNA from HepG2 genomic DNA and cloning the product into pIRES-V5-GFP. CD8-$LDLR_{intracellular}$ (a fusion protein that includes the intracellular tail of LDLR) was amplified from pcDNA3.1-CD8-LDLR (kind gift from Sean Conner, University of Minnesota, MN) and gateway cloned into pDEST47 (22). All plasmids used in mammalian transfection experiments were isolated by $CsCl_2$ gradient centrifugation. The correctness of all constructs used in this study was verified by DNA sequencing.

ELISA. Cell supernatants were cleared by centrifugation at 4°C for 10 min at 10,000 × *g*. PCSK9 concentrations were measured in duplicate in supernatant from HepG2 and Huh7 cells with a SPC900 Quantikine enzyme-linked immunosorbent assay (ELISA) kit (R&D System, Lille, France), as described previously (23).

LDL uptake assays. DyLight 488-labeled LDL was produced as described previously (24). Briefly, to measure LDL uptake, HepG2 cells were washed twice with PBS and incubated with 5 μg/ml DyLight 488-labeled LDL in DMEM supplemented with 0.5% bovine serum albumin (BSA) for 1 h at 37°C or at 4°C as a control. Cells were then washed twice with PBS supplemented with 0.5% BSA and lysed in RIPA buffer. LDL uptake was determined by quantification of the fluorescence signal on a Typhoon imager, and specific LDL uptake into cells is presented as the mean + standard deviation (SD). For confocal imaging, HepG2 cells were grown on glass slides and treated as described above. Subsequently, cells were fixed with paraformaldehyde and stained with 4′,6-diamidino-2-phenylindole (DAPI). A TCS SP8 confocal microscope equipped with a 405-nm laser (for DAPI) and 488-nm laser (for DyLight 488-labeled LDL) and with a 63× objective (Leica Microsystems, Mannheim, Germany) was used.

Statistics. Analysis was done using the Prism software package. Results were evaluated by a *t* test for comparisons of two groups or by one-way analysis of variance (ANOVA) for grouped analysis, and error bars indicate SDs. Symbols for statistically significant *P* values are defined in the figure legends.

RESULTS

We have recently demonstrated that MARCH6 promotes cholesterol-dependent degradation of SQLE but that MARCH6's involvement in oxysterol-stimulated degradation of HMGCR is less clear (16). However, in that study we reported that silencing of MARCH6 significantly elevated basal levels of HMGCR, implicating the involvement of a distinct mechanism (16). We therefore considered the possibility that MARCH6 is involved in transcriptional regulation of HMGCR by SREBP2 (4). As a first step, we tested whether MARCH6 can influence three established SREBP reporters in human hepatocyte-like HepG2 cells. These reporters consist of an artificial tandem SRE (SRE-Luc) and SREs in the context of their SREBP2-regulated proximal promoters (HMGCS-Luc and $LDLR_{4000}$-Luc) (21). The reporters showed

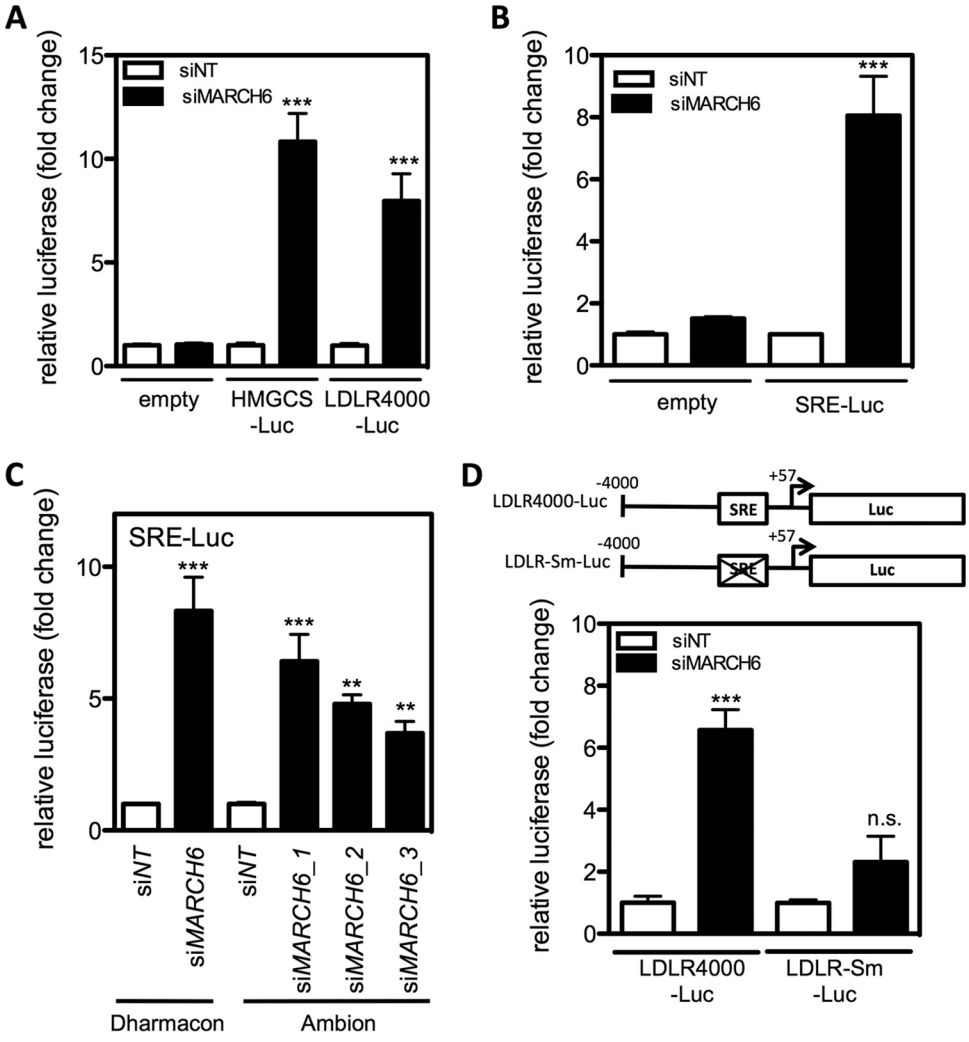

FIG 1 Silencing of MARCH6 increases SREBP-driven reporter constructs in HepG2 cells in an SRE-dependent manner. (A to D) HepG2 cells were transfected with a control siRNA (nontargeting; siNT) or MARCH6 siRNA (siMARCH6), pTK-*Renilla*-luciferase (for transfection normalization), and the indicated firefly luciferase reporter constructs for 48 h. Subsequently, cells were lysed, and dual-luciferase levels were measured. In the experiment shown in panel C, HepG2 cells were transfected in the same manner, but siRNAs from two different suppliers were used (Dharmacon and Ambion) (see Materials and Methods). Results represent the average ± SD from three experiments. **, $P < 0.01$; ***, $P < 0.001$; ns, nonsignificant.

low basal reporter levels under control conditions (Fig. 1A and B). Effective silencing of *MARCH6* in these cells, however, led to a dramatic increase in the transcriptional activity of all three reporters (8- to 10-fold increase) but not of the empty luciferase construct. The effect of MARCH6 knockdown on SRE-luciferase activity was dose dependent (see Fig. S1A in the supplemental material) and was also apparent in Huh7 cells, another hepatocyte-like cell line (see Fig. S1B). Importantly, to rule out the possibility that our observations are an off-target effect of the siRNA we were using, we confirmed that independent single siRNAs targeting *MARCH6* expression also increased the SRE-Luc reporter in HepG2 (Fig. 1C) and Huh7 hepatocytes (see Fig. S1B). The proximal promoter of the LDLR contains an SRE that is essential for its transcriptional regulation by SREBP2 (21, 25). To establish that the transcriptional effect of MARCH6 is SRE dependent, we therefore compared the responses of an LDLR wild-type and an SRE-mutated proximal promoter reporter and found that loss of this element prevents regulation of the reporter by MARCH6 (Fig. 1D). To extend this observation beyond the SRE-based reporter system, we determined the mRNA expression levels of a panel of established SREBP2-regulated genes in hepatocytes. As anticipated, expression of the studied genes increased in response to depletion of cellular cholesterol (Fig. 2). Importantly, expression of *MARCH6* itself was not sensitive to the cellular sterol status (see Fig. S2A in the supplemental material). Silencing *MARCH6* in hepatic cell lines reduced its mRNA levels and increased the protein level of its degradation target, SQLE (see Fig. S2B and C). This also resulted in increased expression of a panel of studied SREBP2 targets in HepG2 cells (Fig. 2), more prominently evident in IHH cells, which is consistent with them being more metabolically responsive (20). Notably, the increase was apparent when cells were cultured in both complete medium and under sterol depletion conditions. In aggregate, these results suggest that *MARCH6* is a negative transcriptional regulator of the SREBP pathway in these cells.

The LDLR is an SREBP2-regulated gene, and accordingly its

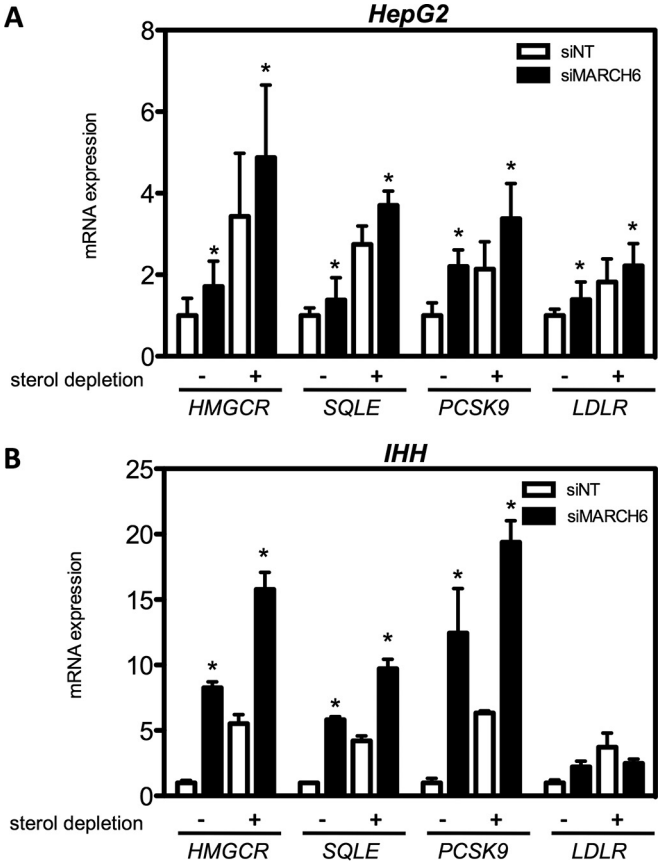

FIG 2 Silencing of MARCH6 increases SREBP2 signaling in hepatocytes. HepG2 and IHH cells were transfected with a control or MARCH6 siRNA for 48 h, after which cells were shifted to sterol-depleted or sterol-containing medium for an additional 24 h. Gene expression was determined by qPCR, and results represent the average ± SD from at least three experiments. *, $P < 0.05$.

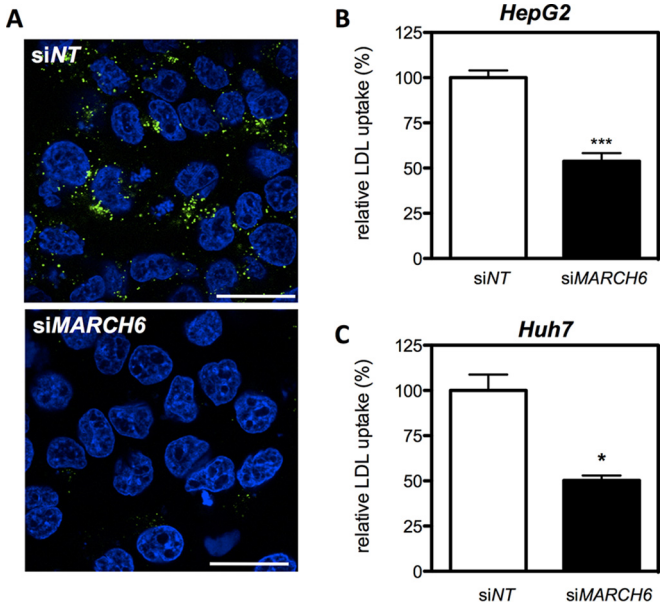

FIG 3 Silencing of MARCH6 decreases LDL uptake in HepG2 and Huh7 cells. HepG2 (A and B) and Huh7 (C) cells were transfected with a control or MARCH6 siRNA for 48 h, after which cells were shifted to sterol depletion medium for an additional 24 h. Subsequently, cells were incubated with 5 μg/ml DyLight 488-labeled LDL for 1 h. Following this cells were fixed, counterstained with DAPI, and imaged by confocal microscopy (A). Representative images are shown (scale bar, 10 μm). (B and C) Alternatively, cells were washed and lysed, and internalized LDL was quantified by measuring fluorescence in total cell lysates. Specific LDL uptake in control cells was set to 100%. Results represent the average ± SD from three experiments. *, $P < 0.01$; ***, $P < 0.001$.

levels are increased in HepG2 and IHH cells following silencing of *MARCH6*. Since the LDLR pathway is the main entry portal for LDL into cells, we expected that the observed increase in *LDLR* mRNA would be accompanied by a concomitant increase in cellular LDL uptake. However, silencing of *MARCH6* substantially decreased uptake of DyLight 488-labeled LDL into HepG2 (Fig. 3A and B) and Huh7 (Fig. 3C) cells as determined by confocal microscopy and quantification of the fluorescence signal in cell lysates. This discrepancy between the *LDLR* mRNA and uptake phenotype was unexpected, leading us to evaluate the level of the LDLR protein in three established hepatocyte cell lines (HepG2, Huh7, and IHH cells) following silencing of *MARCH6*. In agreement with the LDL uptake phenotype, we found that LDLR protein was dramatically reduced following silencing of *MARCH6*, a reduction that could not be overcome by forced activation of the SREBP transcriptional program via sterol depletion (Fig. 4). This result points toward MARCH6 decreasing the level of the LDLR through a posttranscriptional process. To conclusively establish this point, we used HepG2 cells that stably overexpress LDLR-GFP. We have previously shown that as its expression is driven by a constitutive, strong promoter, the levels of the LDLR-GFP fusion protein in these cells is uncoupled from transcriptional regulation by SREBP signaling (10). In these cells, silencing of *MARCH6* reduced the abundance of LDLR-GFP (Fig. 5A and B). Importantly, the effect of *MARCH6* silencing was specific, as abundance of the transferrin receptor remained largely unchanged and that of SQLE increased, as expected.

In addition to reducing the levels of LDLR-GFP, loss of *MARCH6* expression led to a marked redistribution of the protein from the plasma membrane to an intracellular vesicular compartment (Fig. 5C). Given the ER localization of MARCH6, it is difficult to envision a direct scenario that could explain the change in LDLR abundance and localization toward the endolysosomal system. To test if enhanced degradation of the LDLR forms the mechanistic basis for our observations, we tested whether we can reverse the effect of *MARCH6* silencing by blocking the proteasome or the lysosome. Whereas the proteasome inhibitor MG132 had no effect in this assay, the lysosomotropic agent bafilomycin A1 fully rescued the level of the LDLR when *MARCH6* was silenced (Fig. 6).

Involvement of the lysosomal degradation pathway and the acute LDLR redistribution following *MARCH6* silencing are very reminiscent of what occurs following the action of proprotein convertase subtilisin/kexin 9 (PCSK9) or IDOL on the LDLR (10, 26–28). The secreted protein PCSK9 binds the ectodomain of the LDLR, and by a mechanism not yet fully elucidated directs the receptor toward lysosomal degradation by preventing its recycling to the plasma membrane (29). The involvement of PCSK9 in this MARCH6-dependent phenotype may be plausible as PCSK9 is an SREBP2 target (30, 31), and its mRNA is increased by loss of *MARCH6* expression (Fig. 2). To examine this possibility we determined the effect of and siRNA targeting *MARCH6* (si*MARCH6*) on

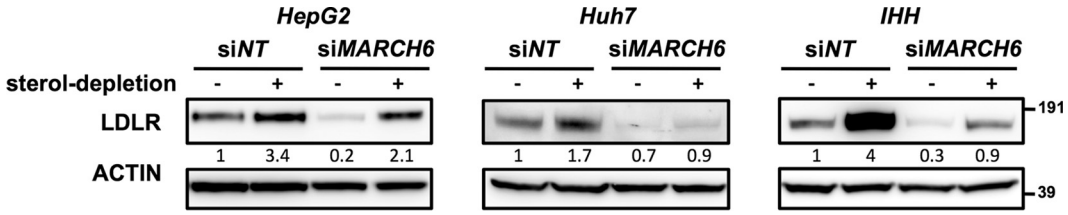

FIG 4 Silencing of MARCH6 decreases abundance of the LDLR in hepatocytes. HepG2, Huh7, and IHH cells were transfected with a control or MARCH6 siRNA for 48 h, after which cells were shifted to sterol-depleted or sterol-containing medium for an additional 24 h. Total cell lysates were immunoblotted as indicated. Immunoblots are representative of three independent experiments, and numbers between the blots indicate the mean LDLR intensity from three independent experiments.

the level of PCSK9 protein in HepG2 and Huh7 cells. Under sterol depletion conditions, when PCSK9 production is turned on, PCSK9 levels in the supernatant were markedly increased in both cell lines in response to loss of *MARCH6* expression (Fig. 7A and B). This increase may be due to enhanced processing and secretion of PCSK9, but intracellular levels of PCSK9 in these cells were insufficient to use them to critically evaluate this possibility. We opted instead for a transfection-based system in HEK293 cells, which allowed us to test the effect of MARCH6 on both processing and secretion of PCSK9. Silencing of *MARCH6* expression in this system was achieved, as evident from the increase in the protein level of the MARCH6 target SQLE, yet neither processing nor secretion of PCSK9 was altered (see Fig. S3A in the supplemental material). Enhanced PCSK9-mediated degradation of the LDLR could be an alternative explanation for the accumulation of PCSK9 in the culture medium following *MARCH6* silencing since the LDLR is required for internalization and clearance of PCSK9. In this scenario, blocking the extracellular activity of PCSK9 should reverse the decrease in the levels of the LDLR induced by silencing of *MARCH6*. For this purpose, we used a PCSK9 blocking antibody, currently under clinical development for lowering LDL cholesterol levels in humans (32). We established that a 100-fold ratio (100 μg/ml) completely reverses degradation of the LDLR induced by 1 μg/ml of recombinant hPCSK9 (see Fig. S3B). This concentration mirrors that measured in culture medium of sterol-depleted HepG2 cells (Fig. 7B). When applied to HepG2 cells, the PCSK9 blocking antibody had a minor effect on the level of LDLR in control cells (Fig. 7C). However, even at the highest

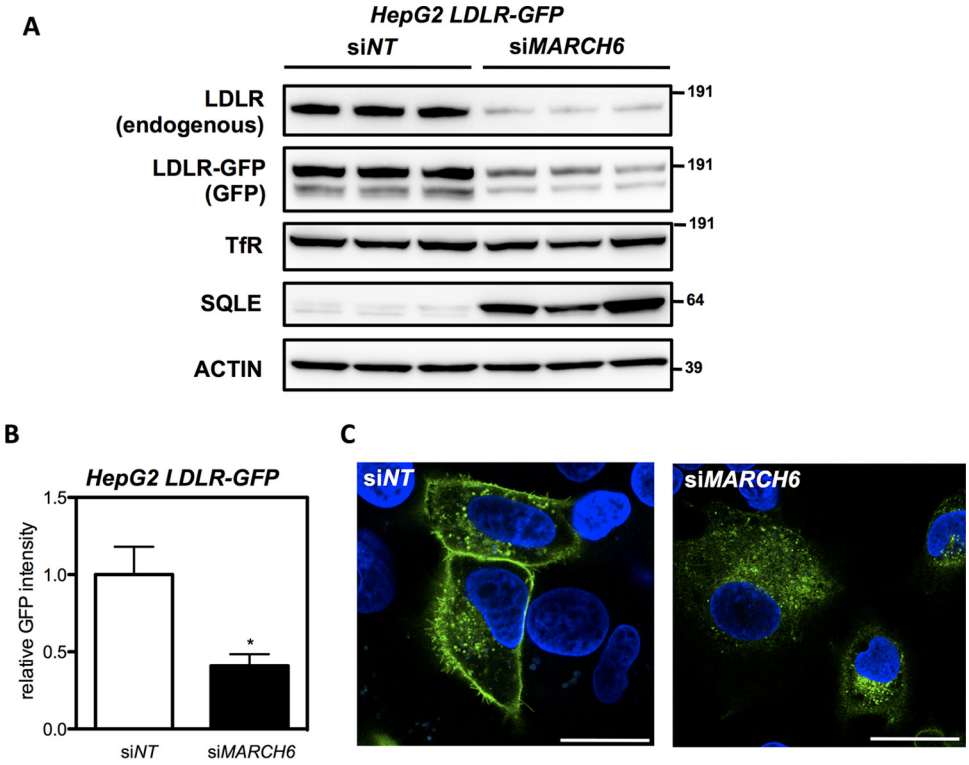

FIG 5 Reduction of LDLR protein by MARCH6 silencing is SREBP independent. HepG2 cells stably expressing LDLR-GFP under the control of a constitutive cytomegalovirus promoter were transfected with control or MARCH6 siRNAs for 48 h. Subsequently, cells were lysed and total cell lysates were immunoblotted as indicated (A). Immunoblots are representative of two independent experiments in triplicate. TfR, transferrin receptor. (B) HepG2 LDLR-GFP cells were treated as described for panel A, and the GFP intensity in total cell lysates was quantified. GFP intensity measured in control cells was set to 1. Results represent the mean ± SD from three experiments. *, $P < 0.05$. (C) Alternatively, cells were fixed, counterstained with DAPI, and imaged by confocal microscopy. Representative images are shown (scale bar, 5 μm).

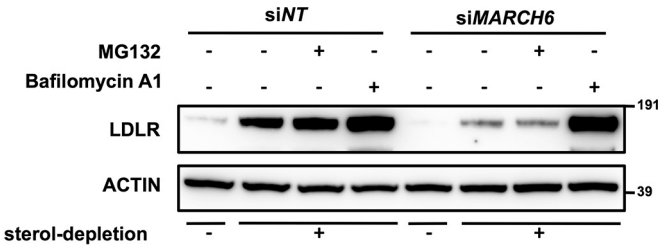

FIG 6 Silencing of MARCH6 promotes lysosomal degradation of the LDLR. HepG2 cells were transfected with a control or MARCH6 siRNA for 48 h, after which cells were shifted to sterol-depleted or sterol-containing medium for an additional 24 h. Subsequently, cells were treated with the proteasome inhibitor MG132 (25 μM) or the lysosomotropic agent bafilomycin A1 (100 nM) for 6 h. Total cell lysates were immunoblotted as indicated. Immunoblots are representative of three independent experiments.

concentration tested (100 μg/ml), the antibody was unable to reverse the *MARCH6*-induced reduction in the level of the LDLR to control levels (Fig. 7C).

As our results rule out the involvement of PCSK9 in the MARCH6-induced phenotype, we considered the involvement of the E3 ligase IDOL, which has also been implicated in lysosomal targeting and degradation of the LDLR (28, 33, 34). In support of IDOL's involvement, we found that the intracellular tail of the LDLR (in the context of a CD8-LDLR chimeric protein) was sufficient to confer *MARCH6* sensitivity (see Fig. S4A in the supplemental material). Furthermore, cosilencing *IDOL* could partially counteract the si*MARCH6*-induced decrease in the level of the chimeric receptor. We therefore tested whether MARCH6 influences the level of *IDOL* mRNA. As previously reported, we found that *IDOL* expression decreased in hepatic cells cultured in sterol depletion medium (Fig. 8A) (10). Unexpectedly, silencing of *MARCH6* resulted in transcriptional induction of *IDOL* mRNA in the three hepatic cell lines tested when they were cultured in complete or sterol-depleted medium. This was not a result of increased mRNA stability since the increase in *IDOL* mRNA was sensitive to the transcription inhibitor actinomycin D (see Fig. S4B).

Our evidence thus far seems to suggest that loss of MARCH6 increases *IDOL* expression and that this induces degradation of the LDLR. To critically test this possibility, we engineered HepG2 cells lacking a functional IDOL using CRISPR/Cas9 technology. In IDOL KO cells, LDLR protein is elevated, and the synthetic LXR ligand GW3695 is unable to promote degradation of the LDLR, confirming that IDOL activity is lost (see Fig. S5A in the supplemental material). In control cells, silencing *MARCH6* increased SQLE protein and decreased the level of the LDLR (Fig. 8B). Consistent with IDOL not being involved in SQLE degradation, silencing of *MARCH6* in IDOL KO cells also elevated the SQLE protein level. However, loss of IDOL prevented the decrease in LDLR abundance following *MARCH6* silencing. Similar results were also obtained by using siRNA technology to cosilence *IDOL* and *MARCH6* in HepG2 and Huh7 cells (see Fig. S5B). Furthermore, in addition to the increase in IDOL, we observed that expression of several other LXR target genes was also increased in HepG2 and IHH cells following silencing of MARCH6 (Fig. 9A and B).

Interestingly, the ability of MARCH6 to control IDOL-dependent degradation may extend beyond the LDLR as we observed that silencing of *MARCH6* also reduced the endogenous levels of another IDOL target, the closely related VLDLR (35), which is not subject to SREBP-dependent regulation (see Fig. S5C in the sup-

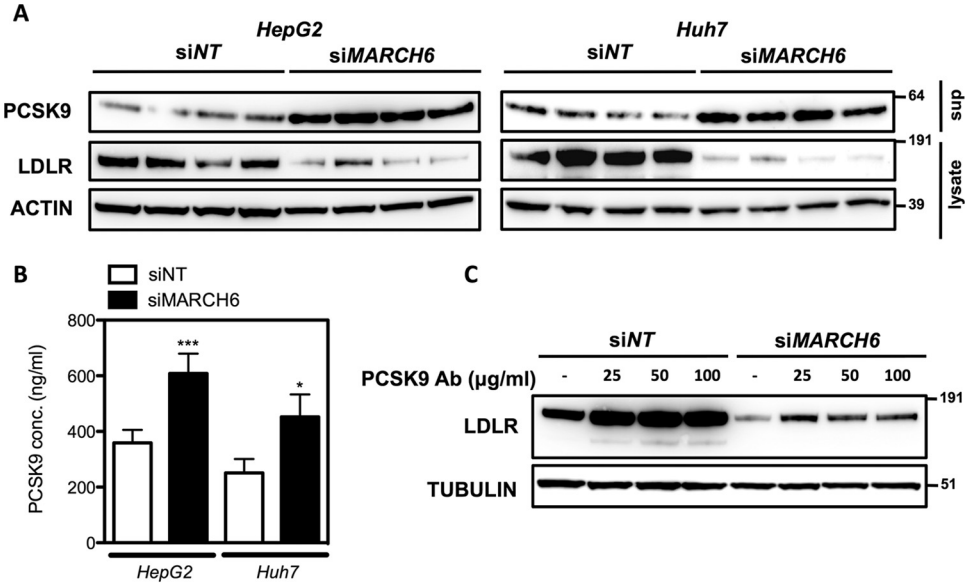

FIG 7 Accumulation of extracellular PCSK9 does not account for the MARCH6-induced degradation of the LDLR. (A and B) HepG2 and Huh7 cells were transfected with a control or MARCH6 siRNA for 48 h, after which cells were shifted to sterol-depleted medium for 24 h. Subsequently, cells were cultured in Opti-MEM for 16 h, supernatants were collected, and total cell lysates were prepared. (A) Total cell lysates and supernatants were immunoblotted as indicated. Immunoblots are representative of three independent experiments. (B) The concentration (concn) of PCSK9 in HepG2 and Huh7 supernatants was determined by ELISA. Results represent the mean ± SD from four (Huh7) or eight (HepG2) experiments. (C) HepG2 cells were transfected as described above and subsequently shifted to sterol-depleted medium for 24 h. Simultaneously, a PCSK9 neutralizing antibody (Ab) (0 to 100 μg/ml) was added to the medium as indicated. Cells were then lysed, and total cell lysates were immunoblotted as indicated. Immunoblots are representative of three independent experiments. Sup, supernatant.

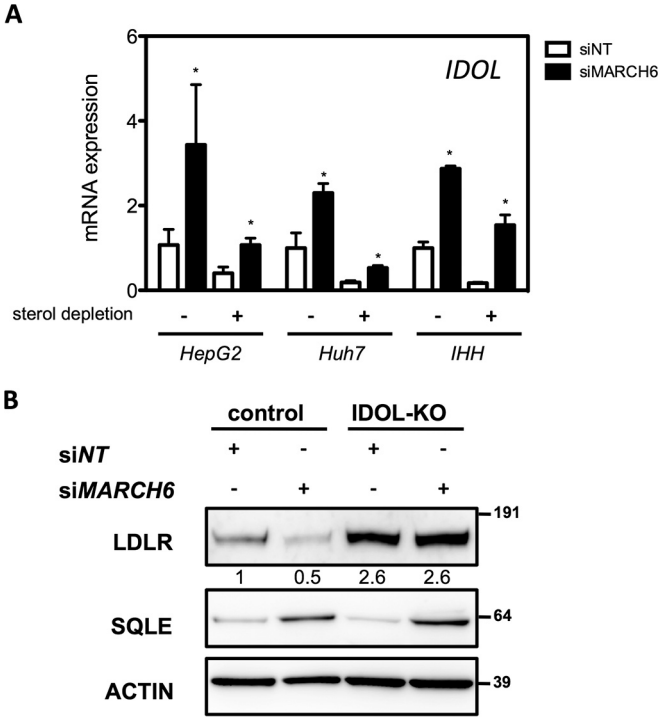

FIG 8 MARCH6-induced degradation of the LDLR in hepatocytes is IDOL dependent. (A) HepG2, Huh7, and IHH cells were transfected with a control or MARCH6 siRNA for 48 h, after which cells were shifted to sterol-depleted- or sterol-containing medium for an additional 24 h. Total RNA was isolated, and gene expression was determined by qPCR ($n = 3$). *, $P < 0.05$. (B) HepG2 control and HepG2 IDOL KO cells were cultured in sterol-containing medium and transfected as described above. Total cell lysates were immunoblotted as indicated. Numbers between the blots represent the mean LDLR intensity of three independent experiments.

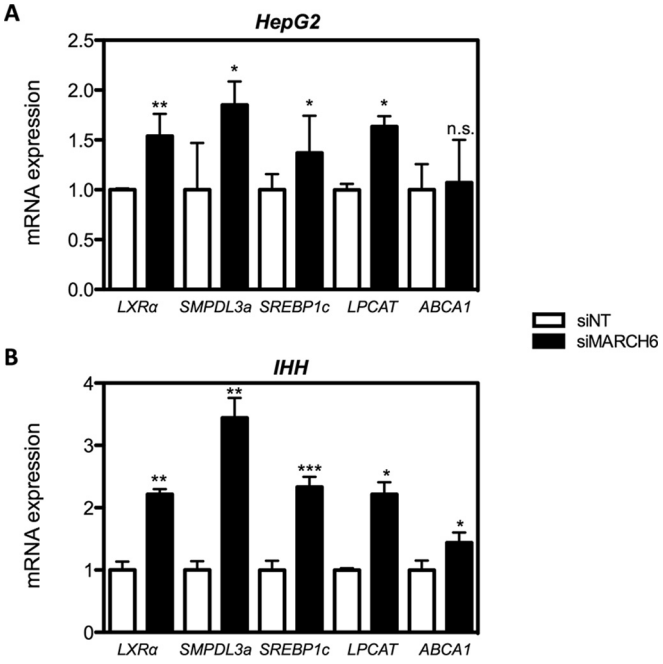

FIG 9 Silencing of MARCH6 increases transcription of LXR-regulated genes. HepG2 and IHH cells were treated as described in the legend to Fig. 2. Gene expression was determined by qPCR, and results represent the average ± SD from at least three experiments *, $P < 0.05$; **, $P < 0.01$; ***, $P < 0.001$; ns, nonsignificant.

plemental material). Our results therefore identify a functional E3 circuit involving MARCH6 and IDOL in controlling the LDLR pathway and lipoprotein uptake.

DISCUSSION

We have recently reported that MARCH6, an ERAD-associated E3 (36), controls stability of SQLE, a rate-limiting enzyme in cholesterol synthesis, in a cholesterol-dependent manner (16). In this study, we investigated the role that MARCH6 plays in maintaining cholesterol homeostasis in hepatocytes. Our main finding is the identification of an unexpected E3 axis functionally coupling MARCH6 and IDOL in the control of lipoprotein uptake via the LDLR pathway.

In our previous study, we reported that in addition to controlling the levels of SQLE, MARCH6 could also regulate the level of HMGCR, thereby positioning it as an important regulator of flux through the mevalonate pathway (16). This regulation was at least in part posttranscriptional as HMGCR protein expressed from a constitutive promoter was also subject to MARCH6-dependent regulation. We demonstrate here that MARCH6 acts as an endogenous inhibitor of SREBP signaling, providing a second mechanism by which MARCH6 can influence HMGCR levels: increased transcription. This is in line with our earlier observation indicating that a major outcome of *MARCH6* loss is an increase in basal levels of HMGCR protein. Activation of SREBPs is a complex process that initiates in the ER and requires the subsequent two-step cleavage of SREBP in the Golgi compartment to release the mature, transcriptionally active, SREBP fragment (7). Given the ER localization of MARCH6 (36), our results are consistent with the idea that MARCH6 promotes degradation of a positive regulator of SREBP processing. However, we think that this is unlikely as we were unable to detect changes in the levels of the SREBP2 precursor protein and in SREBP2 processing by immunoblotting in the studied cells (data not shown). We point out that the transcriptional effect of MARCH6 on the SREBP pathway is limited to cells of hepatic origin and not apparent in a panel of other nonhepatic cell lines, suggesting the involvement of a hepatocyte-specific factor or signaling event. At present, the identity of this factor remains unknown.

The SREBP pathway is activated when cellular cholesterol levels decline as a means to increase cholesterol synthesis and uptake (4). Typically, the SREBP and LXR pathways display reciprocal regulation reflecting their opposing action in cellular cholesterol homeostasis (6, 37). It was therefore unexpected to find that silencing of *MARCH6* also robustly increased the expression of *IDOL*. Additionally, in contrast to the cell-type-specific regulation of SREBP signaling by MARCH6, elevation of *IDOL* expression is more widespread and also apparent to various degrees in cells of nonhepatic origin (e.g., HEK293 and SNB-19 cells). The only transcriptional pathway reported to date to regulate the basal and inducible level of *IDOL* is that controlled by the sterol-sensing LXRs (10). In addition to IDOL, several other LXR-regulated genes also displayed altered expression in response to *MARCH6* silencing. Thus, loss of *MARCH6* in hepatocytes induces a complex cholesterol phenotype in which both the SREBP and LXR pathways are activated. We have previously reported that loss of

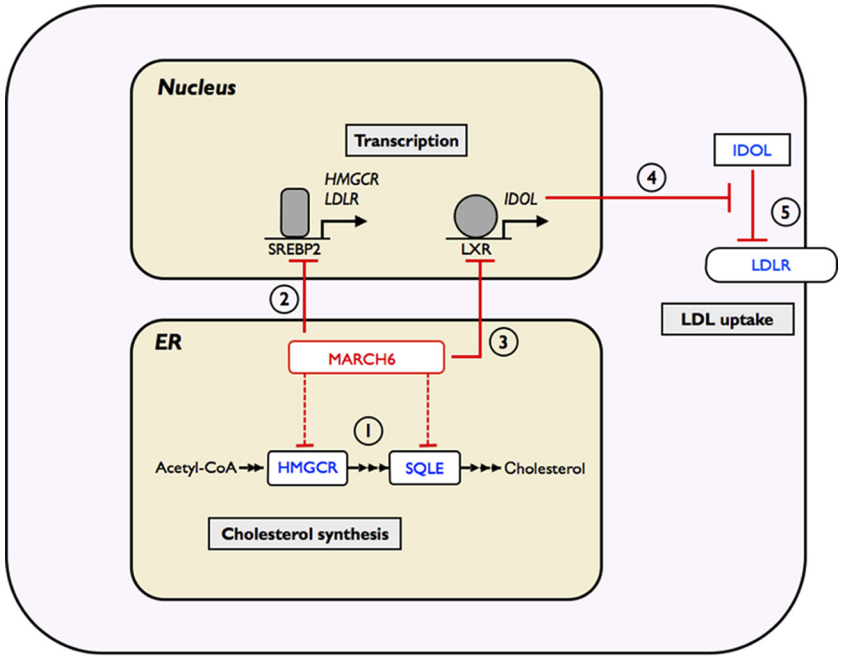

FIG 10 A MARCH6 and IDOL E3 ubiquitin ligase circuit uncouples cholesterol synthesis from lipoprotein uptake in hepatocytes. MARCH6 decreases cholesterol synthesis by (step 1) targeting the key enzymes, HMGCR and SQLE, while also (step 2) reducing SREBP-mediated transcriptional activation of cholesterol synthesis genes and the LDLR. However, (step 3) this decreases production of sterol agonists for LXR and downregulates gene expression of *IDOL*. This in turn (step 4) prevents degradation of the LDLR, thereby (step 5) increasing LDL cholesterol uptake in hepatocytes. Dotted red lines indicate already established targets of the E3 ubiquitin ligase MARCH6 (16). CoA, coenzyme A.

MARCH6 increases metabolic flux through the mevalonate pathway due to dysregulated control of the pathway at the level of the rate-limiting enzyme SQLE (16). As a result, loss of MARCH6 activity enhances production of nonsaponifiable lipids by the mevalonate pathway. Several of the metabolic intermediates and byproducts produced by this pathway, including desmosterol, 24,25-epoxycholesterol, and 27-hydroxycholesterol, are potent endogenous LXR agonists (9, 38–40). Therefore, we speculate that in the absence of MARCH6, the inability to effectively shut down the mevalonate pathway results in activation of the LXR program by these ligands as a means to limit cholesterol accumulation in these cells.

A functional consequence of MARCH6 silencing is a reduction in the ability of cells to take up LDL due to a decrease in LDLR protein. A trivial explanation for this observation could involve enhanced PCSK9-mediated degradation of the LDLR, which is in line with increased *PCSK9* expression and accumulation of secreted PCSK9 in *MARCH6*-silenced cells. However, inhibition of PCSK9-induced degradation of the LDLR using an effective blocking antibody failed to reverse the LDL phenotype. Rather, our results implicate IDOL as the mediator of the MARCH6-induced phenotype. Increased IDOL-mediated degradation of the LDLR also likely explains why secreted PCSK9 accumulates in *MARCH6*-silenced cells; decreased LDLR prevents clearance of PCSK9 via the LDLR pathway, as also suggested previously (41). Hepatic regulation of *IDOL* transcription by LXRs displays a species-specific divergence (42). In human and primate hepatocytes, *IDOL* is robustly regulated by LXR activation, yet this does not occur in rodent hepatocytes for reasons presently unclear. We therefore anticipate that the functional MARCH6-IDOL network will be predominantly active in human hepatocytes. There is increasing genetic evidence from human studies implicating common and rare genetic variation in the *IDOL* locus as a modifier of circulating levels of plasma LDL cholesterol (43, 44). A similar association with *MARCH6* has not been reported yet in genome-wide association studies, and investigations geared toward examining the contribution of rare *MARCH6* variants to this lipid trait are warranted.

In conclusion, we describe here the multifaceted function of MARCH6 in cholesterol homeostasis in hepatocytes, which involves both transcriptional and posttranscriptional mechanisms. We reason that as making cholesterol *de novo* is energetically expensive, the cheapest option for the cell is to derive premade cholesterol by taking up circulating lipoproteins. Our newly identified MARCH6-mediated network uncouples these two modes of cellular cholesterol accretion, sparing cholesterol synthesis while favoring more cholesterol uptake via the LDL receptor (graphically summarized in Fig. 10). This functional E3 circuit linking MARCH6 and IDOL adds an additional, previously unrecognized, feedback mechanism to the control of cellular cholesterol homeostasis.

ACKNOWLEDGMENTS

We kindly thank Sanofi-Regeneron for providing the anti-PCSK9 fully humanized monoclonal antibody alirocumab. We thank members of the Zelcer group, Ben Distel, Eric Reits, and Irith Koster, for their comments and suggestions.

We declare that we have no conflicts of interest.

The funders had no role in study design, data collection and interpretation, or the decision to submit the work for publication. A.J.B. is supported by a grant from the National Health and Medical Research Council (1060515). N.Z. is an Established Investigator of the Dutch Heart Foundation and is supported by a VIDI grant (17.106.355) from the Nether-

lands Organization of Scientific Research and by an ERC Consolidator grant (617376) from the European Research Council.

FUNDING INFORMATION

EC | European Research Council (ERC) provided funding to Noam Zelcer under grant number 617376. Department of Health, Australian Government | National Health and Medical Research Council (NHMRC) provided funding to Andrew John Brown under grant number 10605151. Hartstichting (Dutch Heart Foundation) provided funding to Noam Zelcer under grant number 2013T111. Nederlandse Organisatie voor Wetenschappelijk Onderzoek (NWO) provided funding to Noam Zelcer under grant number 17.106.355.

REFERENCES

1. **Maxfield FR, van Meer G.** 2010. Cholesterol, the central lipid of mammalian cells. Curr Opin Cell Biol **22:**422–429. http://dx.doi.org/10.1016/j.ceb.2010.05.004.
2. **Yokoyama C, Wang X, Briggs MR, Admon A, Wu J, Hua X, Goldstein JL, Brown MS.** 1993. SREBP-1, a basic-helix-loop-helix-leucine zipper protein that controls transcription of the low density lipoprotein receptor gene. Cell **75:**187–197. http://dx.doi.org/10.1016/S0092-8674(05)80095-9.
3. **Hua X, Yokoyama C, Wu J, Briggs MR, Brown MS, Goldstein JL, Wang X.** 1993. SREBP-2, a second basic-helix-loop-helix-leucine zipper protein that stimulates transcription by binding to a sterol regulatory element. Proc Natl Acad Sci U S A **90:**11603–11607. http://dx.doi.org/10.1073/pnas.90.24.11603.
4. **Horton JD, Goldstein JL, Brown MS.** 2002. SREBPs: activators of the complete program of cholesterol and fatty acid synthesis in the liver. J Clin Invest **109:**1125–1131. http://dx.doi.org/10.1172/JCI0215593.
5. **Peet DJ, Turley SD, Ma W, Janowski BA, Lobaccaro JM, Hammer RE, Mangelsdorf DJ.** 1998. Cholesterol and bile acid metabolism are impaired in mice lacking the nuclear oxysterol receptor LXR alpha. Cell **93:**693–704. http://dx.doi.org/10.1016/S0092-8674(00)81432-4.
6. **Zelcer N, Tontonoz P.** 2006. Liver X receptors as integrators of metabolic and inflammatory signaling. J Clin Invest **116:**607–614. http://dx.doi.org/10.1172/JCI27883.
7. **Goldstein JL, DeBose-Boyd RA, Brown MS.** 2006. Protein sensors for membrane sterols. Cell **124:**35–46. http://dx.doi.org/10.1016/j.cell.2005.12.022.
8. **Brown MS, Goldstein JL.** 1986. A receptor-mediated pathway for cholesterol homeostasis. Science **232:**34–47. http://dx.doi.org/10.1126/science.3513311.
9. **Janowski BA, Willy PJ, Devi TR, Falck JR, Mangelsdorf DJ.** 1996. An oxysterol signalling pathway mediated by the nuclear receptor LXR alpha. Nature **383:**728–731. http://dx.doi.org/10.1038/383728a0.
10. **Zelcer N, Hong C, Boyadjian R, Tontonoz P.** 2009. LXR regulates cholesterol uptake through Idol-dependent ubiquitination of the LDL receptor. Science **325:**100–104. http://dx.doi.org/10.1126/science.1168974.
11. **Sharpe LJ, Brown AJ.** 2013. Controlling cholesterol synthesis beyond 3-hydroxy-3-methylglutaryl-CoA reductase (HMGCR). J Biol Chem **288:**18707–18715. http://dx.doi.org/10.1074/jbc.R113.479808.
12. **Jo Y, DeBose-Boyd RA.** 2010. Control of cholesterol synthesis through regulated ER-associated degradation of HMG CoA reductase. Crit Rev Biochem Mol Biol **45:**185–198. http://dx.doi.org/10.3109/10409238.2010.485605.
13. **Song B-L, Sever N, DeBose-Boyd RA.** 2005. Gp78, a membrane-anchored ubiquitin ligase, associates with Insig-1 and couples sterol-regulated ubiquitination to degradation of HMG CoA reductase. Mol Cell **19:**829–840. http://dx.doi.org/10.1016/j.molcel.2005.08.009.
14. **Jo Y, Lee PCW, Sguigna PV, DeBose-Boyd RA.** 2011. Sterol-induced degradation of HMG CoA reductase depends on interplay of two Insigs and two ubiquitin ligases, gp78 and Trc8. Proc Natl Acad Sci U S A **108:**20503–20508. http://dx.doi.org/10.1073/pnas.1112831108.
15. **Gill S, Stevenson J, Kristiana I, Brown AJ.** 2011. Cholesterol-dependent degradation of squalene monooxygenase, a control point in cholesterol synthesis beyond HMG-CoA reductase. Cell Metab **13:**260–273. http://dx.doi.org/10.1016/j.cmet.2011.01.015.
16. **Zelcer N, Sharpe LJ, Loregger A, Kristiana I, Cook ECL, Phan L, Stevenson J, Brown AJ.** 2014. The E3 ubiquitin ligase MARCH6 degrades squalene monooxygenase and affects 3-hydroxy-3-methyl-glutaryl coenzyme A reductase and the cholesterol synthesis pathway. Mol Cell Biol **34:**1262–1270. http://dx.doi.org/10.1128/MCB.01140-13.
17. **Foresti O, Ruggiano A, Hannibal-Bach HK, Ejsing CS, Carvalho P.** 2013. Sterol homeostasis requires regulated degradation of squalene monooxygenase by the ubiquitin ligase Doa10/Teb4. eLife **2:**e00953. http://dx.doi.org/10.7554/eLife.00953.
18. **Sharpe LJ, Cook ECL, Zelcer N, Brown AJ.** 2014. The UPS and downs of cholesterol homeostasis. Trends Biochem Sci **39:**527–535. http://dx.doi.org/10.1016/j.tibs.2014.08.008.
19. **Kikkert M, Doolman R, Dai M, Avner R, Hassink G, van Voorden S, Thanedar S, Roitelman J, Chau V, Wiertz E.** 2004. Human HRD1 is an E3 ubiquitin ligase involved in degradation of proteins from the endoplasmic reticulum. J Biol Chem **279:**3525–3534.
20. **Schippers IJ, Moshage H, Roelofsen H, Müller M, Heymans HS, Ruiters M, Kuipers F.** 1997. Immortalized human hepatocytes as a tool for the study of hepatocytic (de-)differentiation. Cell Biol Toxicol **13:**375–386. http://dx.doi.org/10.1023/A:1007404028681.
21. **Yamaguchi S, Yamane T, Takahashi-Niki K, Kato I, Niki T, Goldberg MS, Shen J, Ishimoto K, Doi T, Iguchi-Ariga SMM, Ariga H.** 2012. Transcriptional activation of low-density lipoprotein receptor gene by DJ-1 and effect of DJ-1 on cholesterol homeostasis. PLoS One **7:**e38144. http://dx.doi.org/10.1371/journal.pone.0038144.
22. **Kang Y-L, Yochem J, Bell L, Sorensen EB, Chen L, Conner SD.** 2013. Caenorhabditis elegans reveals a FxNPxY-independent LDLR internalization mechanism mediated by Epsin1. Mol Biol Cell **24:**308–318. http://dx.doi.org/10.1091/mbc.E12-02-0163.
23. **Lambert G, Petrides F, Chatelais M, Blom DJ, Choque B, Tabet F, Wong G, Rye K-A, Hooper AJ, Burnett JR, Barter PJ, Marais AD.** 2014. Elevated plasma PCSK9 level is equally detrimental for patients with nonfamilial hypercholesterolemia and heterozygous familial hypercholesterolemia, irrespective of low-density lipoprotein receptor defects. J Am Coll Cardiol **63:**2365–2373. http://dx.doi.org/10.1016/j.jacc.2014.02.538.
24. **Motazacker MM, Pirruccello J, Huijgen R, Do R, Gabriel S, Peter J, Kuivenhoven JA, Defesche JC, Kastelein JJP, Hovingh GK, Zelcer N, Kathiresan S, Fouchier SW.** 2012. Advances in genetics show the need for extending screening strategies for autosomal dominant hypercholesterolaemia. Eur Heart J **33:**1360–1366. http://dx.doi.org/10.1093/eurheartj/ehs010.
25. **Wang X, Briggs MR, Hua X, Yokoyama C, Goldstein JL, Brown MS.** 1993. Nuclear protein that binds sterol regulatory element of low density lipoprotein receptor promoter. II. Purification and characterization. J Biol Chem **268:**14497–14504.
26. **Maxwell KN, Fisher EA, Breslow JL.** 2005. Overexpression of PCSK9 accelerates the degradation of the LDLR in a post-endoplasmic reticulum compartment. Proc Natl Acad Sci U S A **102:**2069–2074. http://dx.doi.org/10.1073/pnas.0409736102.
27. **Wang Y, Huang Y, Hobbs HH, Cohen JC.** 2012. Molecular characterization of proprotein convertase subtilisin/kexin type 9-mediated degradation of the LDLR. J Lipid Res **53:**1932–1943. http://dx.doi.org/10.1194/jlr.M028563.
28. **Sorrentino V, Nelson JK, Maspero E, Marques ARA, Scheer L, Polo S, Zelcer N.** 2013. The LXR-IDOL axis defines a clathrin-, caveolae-, and dynamin-independent endocytic route for LDLR internalization and lysosomal degradation. J Lipid Res **54:**2174–2184. http://dx.doi.org/10.1194/jlr.M037713.
29. **Seidah NG.** 2009. PCSK9 as a therapeutic target of dyslipidemia. Expert Opin Ther Targets **13:**19–28. http://dx.doi.org/10.1517/14728220802600715.
30. **Jeong HJ, Lee H-S, Kim K-S, Kim Y-K, Yoon D, Park SW.** 2008. Sterol-dependent regulation of proprotein convertase subtilisin/kexin type 9 expression by sterol-regulatory element binding protein-2. J Lipid Res **49:**399–409.
31. **Dubuc G, Chamberland A, Wassef H, Davignon J, Seidah NG, Bernier L, Prat A.** 2004. Statins upregulate PCSK9, the gene encoding the proprotein convertase neural apoptosis-regulated convertase-1 implicated in familial hypercholesterolemia. Arterioscler Thromb Vasc Biol **24:**1454–1459. http://dx.doi.org/10.1161/01.ATV.0000134621.14315.43.
32. **Lambert G, Chatelais M, Petrides F, Passard M, Thedrez A, RyeK-A, Schwahn U, Gusarova V, Blom DJ, Sasiela W, Marais AD.** 2014. Normalization of low-density lipoprotein receptor expression in receptor defective homozygous familial hypercholesterolemia by inhibition of PCSK9 with alirocumab. J Am Coll Cardiol **64:**2299–2300. http://dx.doi.org/10.1016/j.jacc.2014.07.995.
33. **Scotti E, Calamai M, Goulbourne CN, Zhang L, Hong C, Lin RR, Choi J, Pilch PF, Fong LG, Zou P, Ting AY, Pavone FS, Young SG, Tontonoz P.** 2013. IDOL stimulates clathrin-independent endocytosis and multive-

sicular body-mediated lysosomal degradation of the low-density lipoprotein receptor. Mol Cell Biol **33:**1503–1514. http://dx.doi.org/10.1128/MCB.01716-12.

34. **Sorrentino V, Zelcer N.** 2012. Post-transcriptional regulation of lipoprotein receptors by the E3-ubiquitin ligase inducible degrader of the low-density lipoprotein receptor. Curr Opin Lipidol **23:**213–219. http://dx.doi.org/10.1097/MOL.0b013e3283532947.
35. **Hong C, Duit S, Jalonen P, Out R, Scheer L, Sorrentino V, Boyadjian R, Rodenburg KW, Foley E, Korhonen L, Lindholm D, Nimpf J, van Berkel TJC, Tontonoz P, Zelcer N.** 2010. The E3 ubiquitin ligase IDOL induces the degradation of the low density lipoprotein receptor family members VLDLR and ApoER2. J Biol Chem **285:**19720–19726. http://dx.doi.org/10.1074/jbc.M110.123729.
36. **Hassink G, Kikkert M, van Voorden S, Lee S-J, Spaapen R, van Laar T, Coleman CS, Bartee E, Früh K, Chau V, Wiertz E.** 2005. TEB4 is a C4HC3 RING finger-containing ubiquitin ligase of the endoplasmic reticulum. Biochem J **388:**647–655. http://dx.doi.org/10.1042/BJ20041241.
37. **Bensinger SJ, Bradley MN, Joseph SB, Zelcer N, Janssen EM, Hausner MA, Shih R, Parks JS, Edwards PA, Jamieson BD, Tontonoz P.** 2008. LXR signaling couples sterol metabolism to proliferation in the acquired immune response. Cell **134:**97–111. http://dx.doi.org/10.1016/j.cell.2008.04.052.
38. **Yang C, McDonald JG, Patel A, Zhang Y, Umetani M, Xu F, Westover EJ, Covey DF, Mangelsdorf DJ, Cohen JC, Hobbs HH.** 2006. Sterol intermediates from cholesterol biosynthetic pathway as liver X receptor ligands. J Biol Chem **281:**27816–27826. http://dx.doi.org/10.1074/jbc.M603781200.
39. **Spann NJ, Garmire LX, McDonald JG, Myers DS, Milne SB, Shibata N, Reichart D, Fox JN, Shaked I, Heudobler D, Raetz CRH, Wang EW, Kelly SL, Sullards MC, Murphy RC, Merrill AH, Brown HA, Dennis EA, Li AC, Ley K, Tsimikas S, Fahy E, Subramaniam S, Quehenberger O, Russell DW, Glass CK.** 2012. Regulated accumulation of desmosterol integrates macrophage lipid metabolism and inflammatory responses. Cell **151:**138–152. http://dx.doi.org/10.1016/j.cell.2012.06.054.
40. **Wong J, Quinn CM, Brown AJ.** 2004. Statins inhibit synthesis of an oxysterol ligand for the liver X receptor in human macrophages with consequences for cholesterol flux. Arterioscler Thromb Vasc Biol **24:**2365–2371. http://dx.doi.org/10.1161/01.ATV.0000148707.93054.7d.
41. **Sasaki M, Terao Y, Ayaori M, Uto-Kondo H, Iizuka M, Yogo M, Hagisawa K, Takiguchi S, Yakushiji E, Nakaya K, Ogura M, Komatsu T, Ikewaki K.** 2014. Hepatic overexpression of idol increases circulating protein convertase subtilisin/kexin type 9 in mice and hamsters via dual mechanisms: sterol regulatory element-binding protein 2 and low-density lipoprotein receptor-dependent pathways. Arterioscler Thromb Vasc Biol **34:**1171–1178. http://dx.doi.org/10.1161/ATVBAHA.113.302670.
42. **Hong C, Marshall SM, McDaniel AL, Graham M, Layne JD, Cai L, Scotti E, Boyadjian R, Kim J, Chamberlain BT, Tangirala RK, Jung ME, Fong L, Lee R, Young SG, Temel RE, Tontonoz P.** 2014. The LXR-Idol axis differentially regulates plasma LDL levels in primates and mice. Cell Metab **20:**910–918. http://dx.doi.org/10.1016/j.cmet.2014.10.001.
43. **Teslovich TM, Musunuru K, Smith AV, Edmondson AC, Stylianou IM, Koseki M, Pirruccello JP, Ripatti S, Chasman DI, Willer CJ, Johansen CT, Fouchier SW, Isaacs A, Peloso GM, Barbalic M, Ricketts SL, Bis JC, Aulchenko YS, Thorleifsson G, Feitosa MF, Chambers J, Orho-Melander M, Melander O, Johnson T, Li X, Guo X, Li M, Shin Cho Y, Jin Go M, Jin Kim Y, Lee J-Y, Park T, Kim K, Sim X, Twee-Hee Ong R, Croteau-Chonka DC, Lange LA, Smith JD, Song K, Hua Zhao J, Yuan X, Luan J, Lamina C, Ziegler A, Zhang W, Zee RYL, Wright AF, Witteman JC, Wilson JF, et al.** 2010. Biological, clinical and population relevance of 95 loci for blood lipids. Nature **466:**707–713. http://dx.doi.org/10.1038/nature09270.
44. **Sorrentino V, Fouchier SW, Motazacker MM, Nelson JK, Defesche JC, Dallinga-Thie GM, Kastelein JJP, Kees Hovingh G, Zelcer N.** 2013. Identification of a loss-of-function inducible degrader of the low-density lipoprotein receptor variant in individuals with low circulating low-density lipoprotein. Eur Heart J **34:**1292–1297. http://dx.doi.org/10.1093/eurheartj/ehs472.